Macromolecules

Article

pubs.acs.org/Macromolecules

Scalable Synthesis of Single-Chain Nanoparticles under Mild Conditions

Ashley M. Hanlon,[†] Ruiwen Chen,[†] Kyle J. Rodriguez,[†] Claudia Willis,[†] Jessica G. Dickinson,[†] Mark Cashman,[†] and Erik B. Berda*[,†,‡]

[†]Department of Chemistry and [‡]Material Science Program, University of New Hampshire, Durham, New Hampshire 03824-3598, United States

Supporting Information

ABSTRACT: We present a scalable route to single-chain nanoparticles (SCNP) under mild conditions using intramolecular atom transfer radical coupling (ATRC). Typical methods to SCNP, a class of soft nanomaterials in the sub-10 nm size regime, rely on complicated synthetic techniques, high temperatures unsuitable to fragile functional groups, or ultradilute conditions (solutions less than 1 wt %), all of which greatly complicate scale-up. Our method uses a minimal number of synthetic steps and mild reaction conditions amenable to a wide array of solvents and tolerant to a variety of functional groups. Using this scalable method, gram quantities of nanoparticles in the 5−10 nm size regime are accessible.

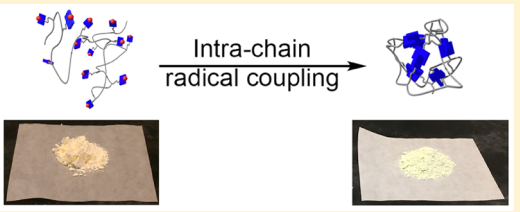

INTRODUCTION

Designing and synthesizing materials that rival Nature's level of control over complex systems on the nanometer length scale remains an important yet elusive research goal. This topic continues to receive considerable research attention based on the technologically transformative potential of biomimetic nanomaterials. One particular subarea of this topic interesting to our group and others involves the manipulation of single polymer chains through intramolecular cross-linking, which induces collapse or "folding" of the polymer chain into an architecturally defined nanoparticle. Interest in such materials, termed "single-chain nanoparticles" (SCNP), continues to increase due to a wide variety of potential applications in catalysis,[1−5] sensors,[6] nanoreactors,[7] and nanomedicine.[8−11] Various types of chemistry including covalent, noncovalent, and metal coordination are demonstrated for the synthesis of SCNP, in which functional groups are directly incorporated into the backbone through the copolymerization of functional monomers or introduced through postpolymerization modifications.[12−18] While current SCNP literature provides a collection of synthetic methodologies to form SCNP, the majority of examples use harsh, dilute conditions that are impractical to scale and result in milligram quantities of nanoparticles.[19−22] The field is in need of strategies that are mild and scalable to illustrate that SCNP are a viable option to obtain nanosized materials. To accomplish this objective, the type of chemistry used as a means to cross-link must be tolerable to practical reaction conditions. We chose to use atom transfer radical coupling (ATRC) as a means to cross-link polymer chains. ATRC conditions are mild, easily scalable, and tolerant to a wide variety of solvent and temperature conditions. Through the use of this type of chemistry multigram quantities of SCNP are feasible.

ATRC is a process similar to atom transfer radical polymerization (ATRP)[23] and copper(0)-mediated polymerizations.[24−26] When using one of these polymerization techniques, a reaction between two polymer chain ends has been considered synthetically useless.[27] However, in a monomer-free environment Cu(I)/Cu(0)-mediated reductive coupling or ATRC is a valuable method to achieve coupled products from bromine-terminated polymers. In ATRC the reaction components are composed of an organic halide species, typically a bromine-terminated polymer, a Cu(I) complex, and Cu(0). Macroradicals are formed at former bromine-terminated sites from the abstraction of the halogen and generation of an oxidized Cu(II) complex. Cu(0) serves as a reducing agent regenerating the Cu(I) catalyst to maximize radical concentration allowing for coupling reactions to occur.[28] ATRC has proven to be a versatile coupling technique with many synthetic applications. Matyjaszewski et al. reported the preparation of alkyoxyamines through coupling of organic radicals with nitroxide traps.[29] Yoshikawa et al.[30] and Sarbu and co-workers[31] prepared polystyrene through coupling of bromine-terminated polymers. Another notable example is the synthesis of macrocycles from dibrominated polymers through ATRC[32] and radical trap-assisted ATRC[33−35] reported by the Tillman group. The versatility and polymer compatibility of ATRC make it an attractive reaction for SCNP synthesis.

Herein we describe an efficient and scalable technique to produce nanoparticles using an approach that is tunable both in monomer design and cross-linking experimental conditions. While the SCNP field continues to grow, it is evident that the majority of examples are lacking complex and tunable synthetic

Received: March 7, 2017

DOI: 10.1021/acs.macromol.7b00497
Macromolecules XXXX, XXX, XXX−XXX

designs, folding control, and scalable methods. Our system allows for easy synthetic tuning of monomers as an attempt to introduce some complexity and tease out ways to access folding control. A continuous addition method offers a route to a scalable method not requiring the use of ultradilute conditions yet current examples use harsh conditions and are only able to reach a 2.5 mg mL^{-1} concentration.[36] We were able to use mild conditions in a continuous addition method and access 10 mg mL^{-1} concentrations through the use of ATRC as a means to cross-link through pendent alkyl bromides (Figure 1). We achieved particle sizes ranging from 5 to 10 nm, an ideal size for potential delivery applications.

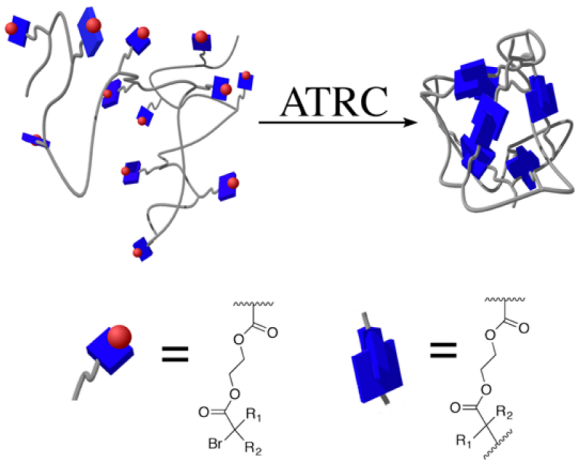

Figure 1. Illustration of SCNP formation using ATRC though pendent monomer units.

MATERIALS AND METHODS

Reagents were obtained from the indicated commercial suppliers and used without further purification unless otherwise stated: Methyl methacrylate and 2-hydroxyethyl methacrylate were filtered through a plug of basic alumina before use. 4-Cyano-4-[(dodecylsulfanylthiocarbonyl)sulfanyl]pentanoic acid was recystallized from methanol and 2,2′-azobisisobutyronitrile from ethanol before use. Dichloromethane (DCM, Fisher Scientific), petroleum ether (Sigma-Aldrich), toluene (Fisher Scientific), tetrahydrofuran (THF, inhibited with BHT, Fisher Scientific), 4-cyano-4-[(dodecylsulfanylthiocarbonyl)-sulfanyl]pentanoic acid (Sigma-Aldrich), 2,2′-azobisisobutyronitrile (Sigma-Aldrich), methyl methacrylate (Sigma-Aldrich), copper(I) bromide (STREM Chemicals Inc.), 2-hydroxyethyl methacrylate (HEMA, Sigma-Aldrich), triethylamine (TEA, Sigma-Aldrich), toluene (EMD Chemicals), 2-bromopropionyl bromide (Sigma-Aldrich), α-bromoisobutryl bromide (Sigma-Aldrich), α-bromophenylacetic acid (Sigma-Aldrich), sodium sulfate (Fisher Scientific), *N,N,N′N″,N″*-pentamethyldiethylenetriamine (PMDETA, Sigma-Aldrich), copper(0) (The Hilman Group Inc.), methanol (Fisher Scientific), 4-(dimethylamino)pyridine (DMAP, Sigma-Aldrich), *N,N′*-dicyclohexylcarbodiimide (DCC, Alfa Aesar), sodium bicarbonate (Fisher Scientific), alumina (activated basic, Alfa Aeser), alumina (neutral, Alfa Aeser), chloroform-d ($CDCl_3$, Cambridge Isotope Laboratories), and *N,N*-dimethylformamide-d_7 (DMF-d_7, Cambridge Isotope Laboratories).

SEC was performed on a Tosoh EcoSEC dual detection (RI and UV) SEC system coupled to an external Wyatt Technologies miniDAWN Treos multiangle light scattering (MALS) detector. Samples were run in THF at 30 °C at a flow rate of 0.35 mL/min. The column set contained one Tosoh TSKgel SuperH2500 (6 × 150 mm) column, one Tosoh TSKgel SuperHM-M (6 × 150 mm) column, one Tosoh TSKgel SuperH3000 (6 × 150 mm) column, one Tosoh TSKgel SuperH4000 (6 × 150 mm), and two Tosoh TSKgel SuperH-L guard columns (4.6 × 3.5 cm). Increment refractive index values (dn/dc) were calculated online assuming 100% mass recovery (RI as the concentration detector) using the Astra 6 software package (Wyatt Technologies) by selecting the entire trace from analyte peak onset to the onset of the solvent peak or flow marker. This method gave the expected values for polystyrene (dn/dc = 0.185, M_n = 30K) when applied to a narrow PDI PS standard supplied by Wyatt. Absolute molecular weights and molecular weight distributions were calculated using the Astra 6 software package. All polymer solutions characterized by SEC were 1.0 mg mL^{-1} and were stirred magnetically for at least 4 h before analysis.

TEM images were recorded using a Zeiss LEO 922 Ω operating at 120 kV with a Gatan Multiscan bottom mount digital camera. Samples were prepared by drop-casting 2 μL of a nanoparticle solution (1 mg mL^{-1}) on to Formvar carbon film coated 400 square mesh copper grids (purchased from Electron Microscopy Sciences) and dried overnight in air while protected from dust.

^1H and ^{13}C NMR spectra were acquired with a Varian Unity INOVA 500 MHz or Varian Mercury 400 MHz spectrometer. Chemical shifts (δ) are reported in parts per million (ppm) relative to tetramethylsilane (TMS). Solvents ($CDCl_3$ and DMF-d_7) contained 0.03% v/v TMS as an internal reference. Peak abbreviations are used as follows: s = singlet, d = doublet, t = triplet, q = quartet, p = pentet, m = multiplet, br = broad, Ar = Aryl. Diffusion-ordered spectroscopy (DOSY) experiments were performed on a Varian UnityINOVA 500 spectrometer running VnmrJ 3.2 and equipped with a 5 mm broadband probe. 20−100 mg of polymer was dissolved in 1 mL of DMF-d_7. All samples were stabilized at 25 °C for 5 min before acquisition. The maximum gradient strength was 0.135 T/m. The pulse sequence used was a DOSY bipolar pulse paired stimulated echo with convection compensation (Dbppste_cc). The following acquisition parameters were employed: diffusion gradient length = 2.0 ms, diffusion delay = 200 ms, gradient stabilization delay = 0.5 ms, gradient steps = 15, and transients = 16. The relative molecular weight (M_w) of each polymer was determined by referencing the diffusion coefficient to a calibration curve generated from polystyrene standards analyzed under the same conditions. DOSY spectra were processed with VnmrJ 3.2 software. Diffusion coefficients were generated by the maximum diffusion projection value.

Synthesis of Monomer 1 (MeBrema). 2-Hydroxyethyl methacrylate (4.90 mL, 0.040 mol), triethylamine (5.63 mL, 0.040 mol), and DCM (30 mL) were added to a dry 100 mL round-bottom flask equipped with a stir bar. The mixture was cooled in an ice bath while stirring, and a solution of 2-bromopropionyl bromide (4.65 mL, 0.044 mol) in DCM (5 mL) was added dropwise through an addition funnel over 15 min. The reaction was kept cold for an additional 45 min before allowing to warm to room temperature. The reaction mixture was kept stirring overnight. The salt byproduct was filtered off, and the filtrate was washed with DI water (25 mL) twice and a saturated sodium bicarbonate solution (25 mL) twice. The organic layer was dried with anhydrous sodium sulfate, and the solvent was removed through rotary evaporation to obtain a yellow oil (9.28 g, 0.035 mol) in an 86.7% yield. ^1H NMR (400 MHz, $CDCl_3$, δ, ppm): 1.83 (d, 3H, CH_3), 1.95 (s, 3H, CH_3), 4.37−4.45 (m, 5H, CH_2), 5.60 (s, 1H, C═CH_2), 6.14 (s, 1H, C═CH_2) (Figure S1). ^{13}C NMR (100 MHz, $CDCl_3$, δ, ppm): 18.5, 21.8, 39.9, 62.2, 63.6, 126.4, 136.0, 167.2, 170.2 (Figure S2).

Synthesis of Monomer 2 (PhBrema). α-Bromophenylacetic acid (6.45 g, 0.030 mol) was put into a 100 mL round-bottom flask equip with a stir bar and dissolved in DCM (75 mL). The resulting solution was cooled in and ice bath. HEMA (1.82 mL, 0.015 mol), DCC (6.19 g, 0.030 mol), and DMAP (0.37 g, 3 mmol) were added, and the mixture was stirred on ice for 10 min. The reaction was then stirred at room temperature overnight. The reaction mixture was filtered, and the filtrate was put through a small plug of silica. The solution was concentrated through rotary evaporation, and the crude product was purified by flash column chromatography using a 4:1 petroleum ether:ethyl acetate eluent to obtain pure product (2.79 g, 8.56 mmol) in a 61% yield. ^1H NMR (400 MHz, $CDCl_3$, δ, ppm): 1.90 (dd, 3H, CH_3), 4.34−4.39 (m, 2H, CH_2), 5.37 (s, 1H, CH), 5.56 (p, 1H, C═

DOI: 10.1021/acs.macromol.7b00497
Macromolecules XXXX, XXX, XXX−XXX

CH_2), 6.06 (p, 1H, C=CH_2), 7.31−7.40 (m, 3H, Ar−H), 7.50−7.60 (m, 2H, Ar−H) (Figure S3). ^{13}C NMR (100 MHz, $CDCl_3$, δ, ppm): 18.5, 46.6, 62.1, 64.1, 126.5, 128.9, 129.1, 129.6, 135.7, 135.9, 168.3, 167.2 (Figure S4).

Synthesis of Monomer 3 (Me_2Brema). 2-Hydroxyethyl methacrylate (3.64 mL, 0.030 mol), triethylamine (4.18 mL, 0.030 mol), and DCM (25 mL) were added to a dry 50 mL round-bottom flask equipped with a stir bar. The mixture was cooled in an ice bath while stirring, and a solution of α-bromoisobutryl bromide (4.08 mL, 0.033 mol) in DCM (5 mL) was added dropwise over 15 min. The reaction was kept cold for an additional 45 min before allowing it to warm to room temperature. The reaction mixture was kept stirring overnight. The salt byproduct was filtered off, and the filtrate was washed with DI water (25 mL) twice. The organic layer was dried with sodium sulfate, and the solvent was removed through rotary evaporation to obtain a yellow oil (7.03 g, 0.025 mol) in an 84% yield. ^{1}H NMR (400 MHz, $CDCl_3$, δ, ppm): 1.94 (s, 6H, CH_3), 1.95 (dd, 3H, CH_3), 4.39−4.46 (m, 4H, CH_2), 5.60 (p, 1H, C=CH_2), 6.14 (p, 1H, C=CH_2) (Figure S5). ^{13}C NMR (100 MHz, $CDCl_3$, δ, ppm): 18.5, 30.9, 55.6, 62.1, 63.7, 126.4, 136.1, 167.3, 171.7 (Figure S6).

Preparation of P1−P5. Methyl methacrylate, functional monomer (MeBrema, Me_2Brema, or PhBrema), 4-cyano-4-[(dodecylsulfanyl-thiocarbonyl)sulfanyl]pentanoic acid and 2,2′-azobis(2-methyl-propionitrile) were dissolved in toluene in a 10 mL Schlenk flask. A magnetic stir bar was added, and the solution was sparged with nitrogen for 30 min. The solution was then heated at 80 °C for 12−20 h and monitored via ^{1}H NMR. The solution was removed from heat, exposed to atmosphere, and allowed to cool to room temperature. The polymer solution was then diluted with THF, precipitated into methanol, and dried under vacuum to afford a white powder.

Preparation of NP1−NP5. To a 10 mL (or 25 mL) Schlenk flask the polymer (50 or 100 mg) was dissolved in toluene (10 or 20 mL). Three freeze−pump−thaw cycles were performed, and the polymer solution was put under nitrogen. In a separate 50 mL (or 100 mL) Schlenk flask PMDETA (10 equiv to functional monomer units), toluene (40 or 80 mL) and a stir bar wrapped in copper(0) were put through four freeze−pump−thaw cycles. This solution was then frozen, and copper(I) bromide (5−10 equiv to functional monomer units) was added. This flask was then evacuated, put under nitrogen, then thawed, and placed in an oil bath at 80 °C. The polymer solution was then added, and the reaction was allowed to stir overnight. The reaction mixture was then opened to air, brought to room temperature, diluted with THF, and put through a plug of neutral alumina twice to remove copper bromide. The nanoparticle was isolated by removing the solvent through rotary evaporation. For large scale reactions the nanoparticle was precipitated into cold methanol twice and then dialyzed in a solution of methanol.

Continuous Addition Procedure. In a 10 mL Schlenk flask the polymer (100 mg or 1 g) was dissolved in toluene (1 or 10 mL). Three freeze−pump−thaw cycles were performed, and the polymer solution was put under nitrogen. In a separate 50 mL (or 100 mL) Schlenk flask PMDETA (1−5 equiv to functional monomer units), toluene (9 or 90 mL) and a stir bar wrapped in copper(0) were put through four freeze−pump−thaw cycles. This solution was then frozen, and copper(I) bromide (1−5 equiv to functional monomer units) was added. This flask was evacuated, put under nitrogen, then thawed, and placed in an oil bath at 80 °C. The polymer solution was then added at a rate of 1 mL/h using a syringe pump for a final concentration of 10 mg/mL. The reaction was allowed to stir overnight. The reaction mixture was then opened to air, brought to room temperature, diluted with THF, and put through a plug of neutral alumina to remove copper bromide. The nanoparticle was then precipitated into cold methanol to yield a light green/blue powder.

RESULTS AND DISCUSSION

Monomer Design. We sought to not only illustrate the efficiency of ATRC-based SCNP synthesis but also deleniate what structural parameters best promote efficient intrachain coupling between active pendent groups. As ATRC mirrors the termination events observed in a typical radical chain polymerization, we examined a range of monomers with different propensities to terminate by coupling or disproportionation (Figure 2). To these ends we synthesized three

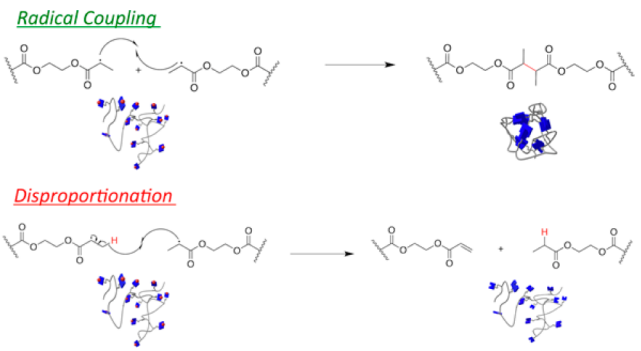

Figure 2. Representation of two possible routes during ATRC: radical coupling and disproportionation.

monomers: MeBrema, Me_2Brema, and PhBrema, each having differing radical-site characteristics (Scheme 1). The PhBrema

Scheme 1. Three ATRC-Active Monomers and the Resulting Radicals Formed under ATRC Conditions

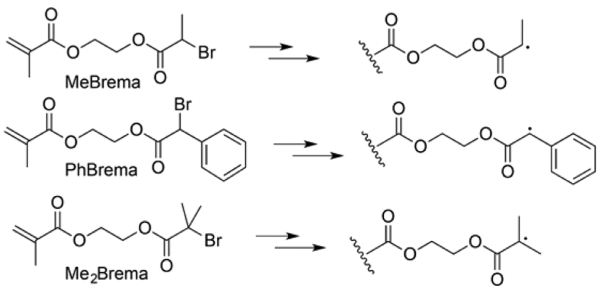

monomer has no possibility to disproportionate due to a lack of α-hydrogens, while the MeBrema and Me_2Brema have three or six abstractable α-hydrogens providing different rates of disproportionation. This design permits systematic testing of the effect the termination mechanism has on SCNP formation.

Polymer Synthesis. We obtained linear polymer precursors with an ATRC-active monomer and methyl methacrylate as a comonomer using reversible addition−fragmentation chain transfer (RAFT) polymerization (Scheme 2). RAFT polymerization was chosen not only for its excellent control over molecular weight, narrow molecular weight distribution, and monomer tolerance but also because it results in end groups that are unreactive under ATRC conditions.[37] We synthesized a

Scheme 2. RAFT Copolymerization of MeBrema, PhBrema, or Me_2Brema and Methyl Methacrylate Followed by ATRC Nanoparticle Formation

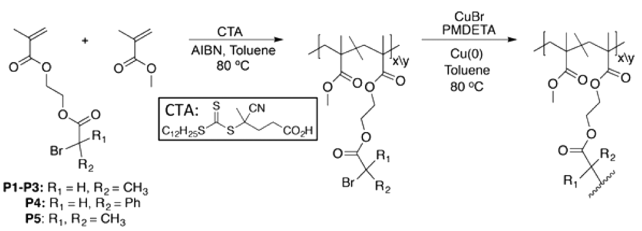

DOI: 10.1021/acs.macromol.7b00497
Macromolecules XXXX, XXX, XXX−XXX

series of three polymers with approximately 10, 20, and 50% incorporation of MeBrema as well as two additional polymers with around 10% incorporation of an ATRC-active monomer, one with PhBrema and the other with Me_2Brema. All polymers exhibit narrow molecular weight distributions with polydispersity indices ranging from 1.04 to 1.16 and similar molecular weights of 14−30 kDa (Table 1). The ^{1}H NMR spectra for each polymer show distinguishable signals from the particular ATRC-active monomer allowing for easy calculations of percent incorporations (Figures S7, S9, S11, S13, and S15).

Table 1. SEC Data for Polymers P1−P5 and Corresponding Nanoparticles NP1−NP5

sample	M_n[a] [kDa]	M_w[a] [kDa]	PDI[a]	comonomer incorporation	peak retention time[b] [min]
P1	18.9	20.4	1.08	10.7	12.5
NP1	15.7	16.1	1.03		12.6
P2	22.4	23.3	1.04	28.3	12.3
NP2	21.7	22.3	1.03		12.7
P3	18.8	20.2	1.07	53.9	12.5
NP3	11.2	13.0	1.16		12.8
P4	26.3	30.0	1.14	11.9	12.3
NP4	29.5	29.9	1.01		12.7
P5	14.1	15.2	1.08	12.5	12.8
NP5	13.6	14.3	1.06		12.5

[a]Obtained using triple detection SEC. See the Supporting Information for more details. [b]Calculated from MALS detector trace.

Nanoparticle Synthesis. We adopted the following nomenclature in this work: Each parent linear polymer is assigned a number and given the prefix (P). The nanoparticles are labeled NP with the following number indicating which polymer precursor was used.

Single-chain nanoparticles formed by introducing the linear polymer precursors to ATRC conditions, as shown in Scheme 2. Since nanoparticle formation requires dilute solutions (1 mg mL^{-1}) to favor intramolecular cross-linking and reduce the probability for intermolecular interactions, we used a 5−10-fold excess of CuBr, PMDETA, and Cu(0). For each example, nanoparticle formation resulted in a slight decrease in absolute molecular weight as determined by SEC-MALS (Table 1), which is feasible due to the loss of multiple pendent bromines during cross-linking. Consistently observed was an increase in retention time from parent polymer to nanoparticle. We found an exception to this trend with **NP3** in which the SEC trace did not show a clean shift to longer retention time. We attribute this observation to disproportionation events and intermolecular reactions due to a higher incorporation of ATRC-active monomer in the linear analogue. For each successful SCNP synthesis retention time increases are observed in SEC when going from linear polymer to SCNP, consistent with a reduction in hydrodynamic radius (Figures 3 and 4). We evaluated the efficiency of nanoparticle synthesis through a comparison of polymers with the three different ATRC-active monomers, all at approximately 10% incorporation. The polymer containing the PhBrema monomer experienced the largest and cleanest shift to a longer retention time, which is expected since this particular monomer has no chance to participate in disproportionation reactions. The polymer containing MeBrema shows a small shift to longer retention time, while the precursor containing Me_2Brema experiences a broadening in the SEC trace from **P5** to **NP5**, likely due to disproportionation events. When using Me_2Brema as the ATRC-active monomer, evidence of disproportionation is seen in ^{1}H NMR spectra (Figure 5). Figure 3 gives a comparison of various incorporations of MeBrema monomer within the parent polymer to elucidate the effect on nanoparticle formation. Increasing the incorporation of MeBrema from approximately 10 to 20% shows a larger shift to a longer retention time, which is thought to be due to an increase in the amount of cross-links leading to a more compact nanoparticle. Increasing the incorporation to approximately 50% of the MeBrema monomer resulted in a shift to a longer

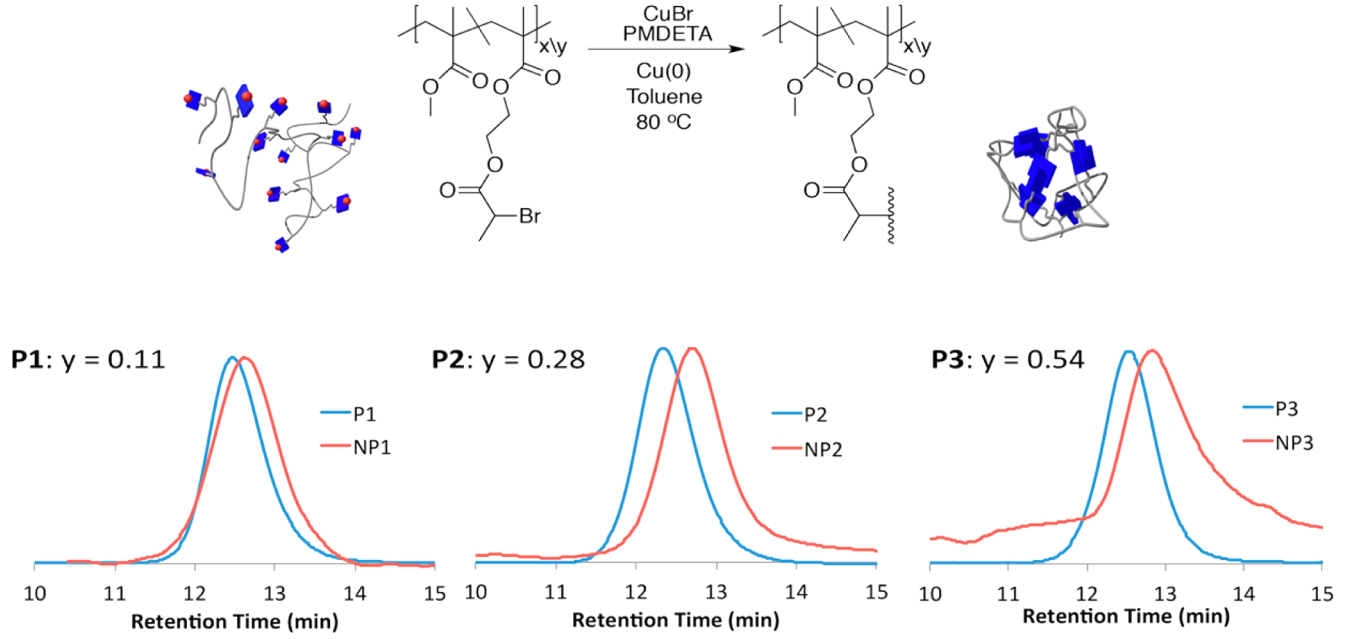

Figure 3. MALS-SEC trace overlays from parent polymer to nanoparticle, comparing the effect of different incorporations of the MeBrema monomer.

DOI: 10.1021/acs.macromol.7b00497
Macromolecules XXXX, XXX, XXX−XXX

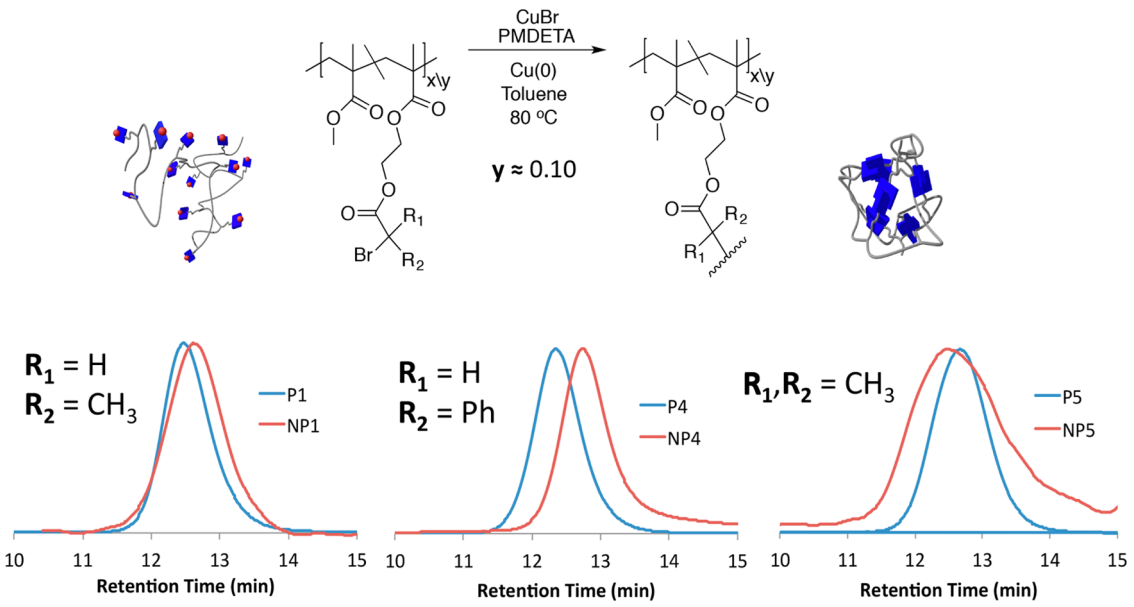

Figure 4. MALS-SEC trace overlays from parent polymer to nanoparticle, comparing the effect of using different ATRC-active monomers.

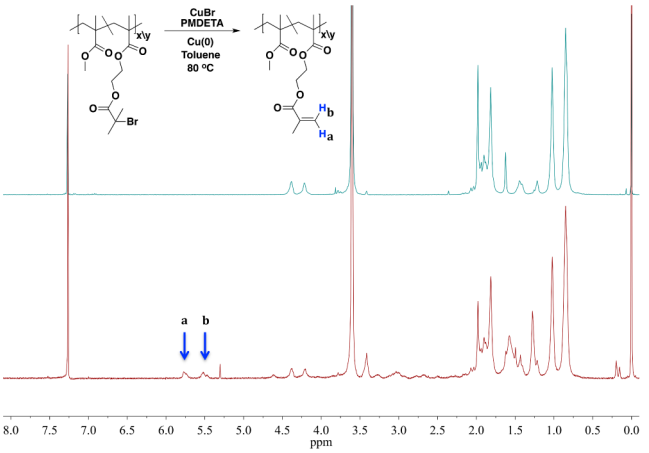

Figure 5. ^{1}H NMR spectra overlay of Me_2Brema containing polymer (top) and the polymer after introduction to ATRC conditions resulting in disproportionation (bottom).

retention time for the majority of the trace, yet there is likely both interchain interactions as well as some disproportionation events indicated by the aggregations seen at a shorter retention time.

Spectroscopic evidence confirmed cross-link formation. Figure 6B illustrates the changes in the ^{1}H NMR spectra going from **P2** to **NP2**. Specifically the proton resonance of the hydrogen labeled **a** in the parent polymer shifts upfield from 4.5 to 2.5 ppm when the chain is collapsed into a nanoparticle (**a**′). Desheilding of that particular proton occurs in the parent polymer since it is adjacent to a bromine, once folding occurs through ATRC that bromine is lost resulting in a shift of the resonance to a lower ppm. Although less obvious, the same can be said for the methyl proton resonance labeled **e** and **e**′ which shifts from 1.9 to 1.2 ppm from **P2** to **NP2**, respectively.

In addition to the ^{1}H NMR evidence of SCNP formation, DOSY experiments provided quantitative information on the reduction in hydrodynamic volume. DOSY experiments directly determine diffusion coefficients of a polymer in solution, which are inversely proportional to the hydrodynamic radii. This in turn provides convincing evidence of intramolecular collapse via the observed increase in the diffusion coefficient of SCNP relative to their parent polymers.[38,39] As shown in Figure 6A, from parent polymer to nanoparticle there is an increase in the diffusion coefficient as well as a decrease in the relative molecular weight when compared to polystyrene standards. Through application of a version of the Stokes−Einstein equation the diffusion coefficients obtained from DOSY experiments provide hydrodynamic radii of 4.5 and 3.5 nm for the parent polymer **P2** and corresponding nanoparticle **NP2**, respectively; these data are indicative of nanoparticle formation.[40,41] Lastly, transmission electron microscopy (TEM) provided visual evidence of nanoparticle formation (Figure 7B), displaying particles with sizes consistent with DOSY values.

One of the major challenges faced in the SCNP field is the development of scalable methods. Dilute polymer concentrations are typically required for most SCNP syntheses. An elegant solution to this problem was first demonstrated by Hawker and co-workers using a continuous addition technique, applied to a SCNP system using the intramolecular dimerization of benzocyclobutene groups at high temperatures.[36] Using the thermal ring-opening and subsequent cycloaddition of 4-vinylbenzocyclobutene as active units, intrachain cross-linking was induced by adding a concentrated polymer solution slowly to hot solvent, eventually reaching a final nanoparticle concentration of 2.5 mg mL^{-1}. The obvious drawback here is the use of solvents at 200 °C. Harth and co-workers developed a way to bring this activation temperature down to 120 °C.[36] While this is a great improvement, it still severely limits the scope of possible reaction conditions. Applying this continuous addition strategy to the ATRC chemistry we describe here circumvents these issues owing to its tolerance to a wide variety of solvent and temperature conditions. This method required less solvent; it also required less equivalents of CuBr, PMDETA, and Cu(0) and allowed for practical targeting of larger scale reactions that are unreasonable at high dilutions due to the requirement of degassing the system using a freeze−pump−thaw technique. By reason for the success of forming **NP2** from **P2**, this polymer was used in

DOI: 10.1021/acs.macromol.7b00497
Macromolecules XXXX, XXX, XXX−XXX

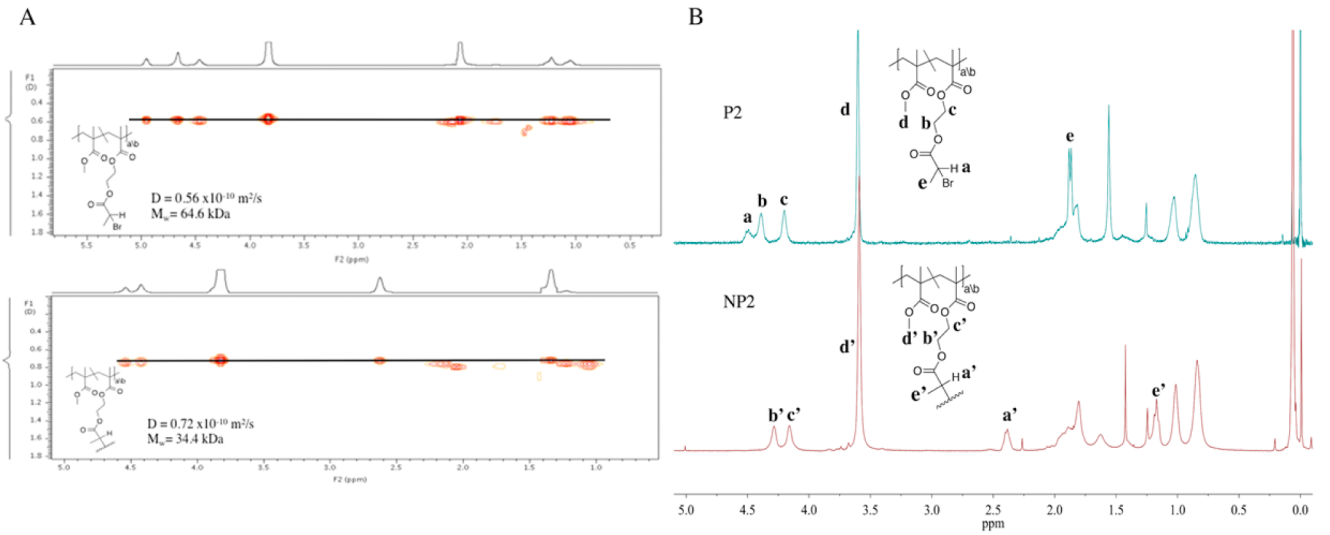

Figure 6. (A) DOSY experiments in DMF-d_7 at 25 °C before cross-linking of linear polymer precursor and corresponding nanoparticle (**P2**, **NP2**). Apparent molecular weight values are based on polystyrene standards. (B) ^{1}H NMR overlay spectrum of polymer **P2** and nanoparticle **NP2**.

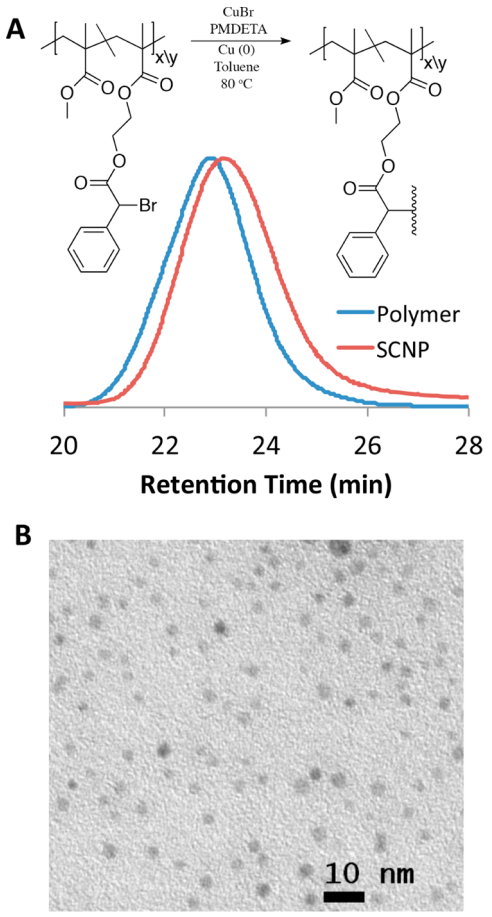

Figure 7. (A) MALS-SEC traces overlay of PhBrema polymer precursor and nanoparticle (B) TEM Image of nanoparticles.

initial continuous addition studies. As seen in Figure 8, from polymer (**CAP1**) to nanoparticle (**CANP1**) there is a significant increase in retention time, indicating a large reduction in size. While the change in retention time is much larger than that seen for the analogous ultradilute reaction (**NP2**), there is also an increase in the PDI indicating a loss of uniformity in the particles obtained. A larger PDI can be

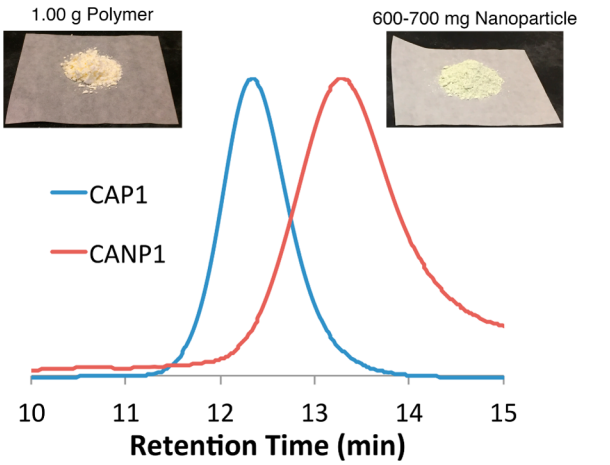

Figure 8. MALS-SEC traces overlay of polymer precursor (**CAP1**) and nanoparticle (**CANP1**) through a continuous addition method.

attributed to the increased concentration from 1 to 10 mg mL^{-1}. The increase in PDI is a small loss compared to the benefits of utilizing a continuous addition method. This continuous addition method was repeatable, as seen in the Supporting Information, and when using 1 g quantities of parent polymer 600−700 mg of nanoparticle could be isolated. The least successful nanoparticle synthesis was produced from Me_2Brema-containing polymers; therefore, to test the effect of continuous addition, another Me_2Brema polymer was synthesized (Figures S22 and S23) and nanoparticle formation was induced using a continuous addition approach. While only a slight increase in retention time was shown (Figure S25), unlike the results from dilute conditions, there was no shift to a shorter retention time or broadening of the SEC trace. In addition, the ^{1}H NMR of the nanoparticle shows no evidence of disproportionation (Figure S26), and DOSY results indicate a reduction in size from polymer to nanoparticle (Figure S27).

CONCLUSIONS

We have developed a method for fabricating single-chain nanoparticles through intramolecular atom transfer radical coupling of pendent alkyl or benzyl bromide moieties on

DOI: 10.1021/acs.macromol.7b00497
Macromolecules XXXX, XXX, XXX−XXX

methacrylate-based polymers. This study offers a new route to SCNP under mild and tunable conditions. Traditional dilute solutions (1 mg mL^{-1}) as well as more concentrated solutions (10 mg mL^{-1}) using a continuous addition method are possible with this system. Consistently we achieved near gram quantities of nanoparticles through the continuous addition method. A major limitation in the SCNP field is the development of scalable methods. The results of this study indicate that with further investigation multigram quantities of nanoparticles are possible. Current SCNP literature provides a variety of types of chemistries used for cross-linking reactions, although it lacks an abundant amount of strategies that are tunable by altering the type of pendent groups or reaction conditions. Simply synthetic tuning of ATRC-active monomers accesses radical sites with various electronic and structural properties affecting the resulting nanoparticles formed from intramolecular cross-linking. ATRC chemistry is tolerable in a wide variety of solvents and temperature conditions. Through the use of this chemistry the type of reagents used could potentially significantly affect the rate of nanoparticle formation. Specifically the rate of coupling could be tuned by varying the type of ligand used due to its ability to affect the rate of radical formation. We are currently testing the versatility of this method through both monomer design and reaction conditions.

■ ASSOCIATED CONTENT

Supporting Information

The Supporting Information is available free of charge on the ACS Publications website at DOI: 10.1021/acs.macromol.7b00497.

Experimental details, GPC traces, TEM images, and NMR spectra (PDF)

■ AUTHOR INFORMATION

Corresponding Author

*(E.B.B.) E-mail Erik.berda@unh.edu.

Notes

The authors declare no competing financial interest.

■ ACKNOWLEDGMENTS

Data were collected on the 400 and 500 MHz NMR within the University Instrumentation Center (UIC) at the University of New Hampshire in Durham, NH. The authors thank the Army Research Office for financial support through Award W911NF-14-1-0177 and NIST for support through Award 70NANB15H060.

■ REFERENCES

(1) Perez-Baena, I.; Barroso-Bujans, F.; Gasser, U.; Arbe, A.; Moreno, A. J.; Colmenero, J.; Pomposo, J. A. Endowing Single-Chain Polymer Nanoparticles with Enzyme-Mimetic Activity. *ACS Macro Lett.* **2013**, *2*, 775−779.

(2) Terashima, T.; Mes, T.; De Greef, T. F. A.; Gillissen, M. A. J.; Besenius, P.; Palmans, A. R. A.; Meijer, E. W. Single-Chain Folding of Polymers for Catalytic Systems in Water. *J. Am. Chem. Soc.* **2011**, *133*, 4742−4745.

(3) Artar, M.; Terashima, T.; Sawamoto, M.; Meijer, E. W.; Palmans, A. R. A. Understanding the catalytic activity of single-chain polymeric nanoparticles in water. *J. Polym. Sci., Part A: Polym. Chem.* **2014**, *52*, 12−20.

(4) Huerta, E.; Stals, P. J. M.; Meijer, E. W.; Palmans, A. R. A. Consequences of Folding a Water-Soluble Polymer Around an Organocatalyst. *Angew. Chem., Int. Ed.* **2013**, *52*, 2906−2910.

(5) Sanchez-Sanchez, A.; Asenjo-Sanz, I.; Buruaga, L.; Pomposo, J. A. Naked and Self-Clickable Propargylic-Decorated Single-Chain Nanoparticle Precursors via Redox-Initiated RAFT Polymerization. *Macromol. Rapid Commun.* **2012**, *33*, 1262−1267.

(6) Gillissen, M. A. J.; Voets, I. K.; Meijer, E. W.; Palmans, A. R. A. Single chain polymeric nanoparticles as compartmentalised sensors for metal ions. *Polym. Chem.* **2012**, *3*, 3166−3174.

(7) He, J.; Tremblay, L.; Lacelle, S.; Zhao, Y. Preparation of polymer single chain nanoparticles using intramolecular photodimerization of coumarin. *Soft Matter* **2011**, *7*, 2380−2386.

(8) Perez-Baena, I.; Loinaz, I.; Padro, D.; Garcia, I.; Grande, H. J.; Odriozola, I. Single-chain polyacrylic nanoparticles with multiple Gd(III) centers as potential MRI contrast agents. *J. Mater. Chem.* **2010**, *20*, 6916−6922.

(9) Sanchez-Sanchez, A.; Akbari, S.; Etxeberria, A.; Arbe, A.; Gasser, U.; Moreno, A. J.; Colmenero, J.; Pomposo, J. A. "Michael" Nanocarriers Mimicking Transient-Binding Disordered Proteins. *ACS Macro Lett.* **2013**, *2*, 491−495.

(10) Passarella, R. J.; Spratt, D. E.; van der Ende, A. E.; Phillips, J. G.; Wu, H.; Sathiyakumar, V.; Zhou, L.; Hallahan, D. E.; Harth, E.; Diaz, R. Targeted Nanoparticles That Deliver a Sustained, Specific Release of Paclitaxel to Irradiated Tumors. *Cancer Res.* **2010**, *70*, 4550−4559.

(11) Hariri, G.; Edwards, A. D.; Merrill, T. B.; Greenbaum, J. M.; van der Ende, A. E.; Harth, E. Sequential Targeted Delivery of Paclitaxel and Camptothecin Using a Cross-Linked "Nanosponge" Network for Lung Cancer Chemotherapy. *Mol. Pharmaceutics* **2013**, *11*, 265−275.

(12) Lyon, C. K.; Prasher, A.; Hanlon, A. M.; Tuten, B. T.; Tooley, C. A.; Frank, P. G.; Berda, E. B. A brief user's guide to single-chain nanoparticles. *Polym. Chem.* **2015**, *6*, 181−197.

(13) Hanlon, A. M.; Lyon, C. K.; Berda, E. B. What Is Next in Single-Chain Nanoparticles? *Macromolecules* **2016**, *49*, 2−14.

(14) Aiertza, M. K.; Odriozola, I.; Cabanero, G.; Grande, H. J.; Loinaz, I. Single-chain polymer nanoparticles. *Cell. Mol. Life Sci.* **2012**, *69*, 337−346.

(15) Altintas, O.; Barner-Kowollik, C. Single chain folding of synthetic polymers by covalent and non-covalent interactions: current status and future perspectives. *Macromol. Rapid Commun.* **2012**, *33*, 958−971.

(16) Sanchez-Sanchez, A.; Perez-Baena, I.; Pomposo, J. A. Advances in click chemistry for single-chain nanoparticle construction. *Molecules* **2013**, *18*, 3339−3355.

(17) Huo, M.; Wang, N.; Fang, T.; Sun, M.; Wei, Y.; Yuan, J. Single-chain polymer nanoparticles: Mimic the proteins. *Polymer* **2015**, *66*, A11−A21.

(18) Altintas, O.; Barner-Kowollik, C. Single-Chain Folding of Synthetic Polymers: A Critical Update. *Macromol. Rapid Commun.* **2016**, *37*, 29−46.

(19) Prasher, A.; Loynd, C. M.; Tuten, B. T.; Frank, P. G.; Chao, D.; Berda, E. B. Efficient fabrication of polymer nanoparticles via sonogashira cross-linking of linear polymers in dilute solution. *J. Polym. Sci., Part A: Polym. Chem.* **2016**, *54*, 209−217.

(20) Lyon, C. K.; Hill, E. O.; Berda, E. B. Zipping Polymers into Nanoparticles via Intrachain Alternating Radical Copolymerization. *Macromol. Chem. Phys.* **2016**, *217*, 501−508.

(21) Jiang, J.; Thayumanavan, S. Synthesis and Characterization of Amine-Functionalized Polystyrene Nanoparticles. *Macromolecules* **2005**, *38*, 5886−5891.

(22) Mecerreyes, D.; Lee, V.; Hawker, C. J.; Hedrick, J. L.; Wursch, A.; Volksen, W.; Magbitang, T.; Huang, E.; Miller, R. D. A Novel Approach to Functionalized Nanoparticles: Self-Crosslinking of Macromolecules in Ultradilute Solution. *Adv. Mater.* **2001**, *13*, 204−208.

(23) Wang, J.-S.; Matyjaszewski, K. Controlled/"living" radical polymerization. atom transfer radical polymerization in the presence of transition-metal complexes. *J. Am. Chem. Soc.* **1995**, *117*, 5614−5615.

DOI: 10.1021/acs.macromol.7b00497
Macromolecules XXXX, XXX, XXX−XXX

(24) Matyjaszewski, K.; Coca, S.; Gaynor, S. G.; Wei, M.; Woodworth, B. E. Zerovalent Metals in Controlled/"Living" Radical Polymerization. *Macromolecules* **1997**, *30*, 7348−7350.
(25) Percec, V.; Popov, A. V.; Ramirez-Castillo, E.; Monteiro, M.; Barboiu, B.; Weichold, O.; Asandei, A. D.; Mitchell, C. M. Aqueous Room Temperature Metal-Catalyzed Living Radical Polymerization of Vinyl Chloride. *J. Am. Chem. Soc.* **2002**, *124*, 4940−4941.
(26) Percec, V.; Guliashvili, T.; Ladislaw, J. S.; Wistrand, A.; Stjerndahl, A.; Sienkowska, M. J.; Monteiro, M. J.; Sahoo, S. Ultrafast Synthesis of Ultrahigh Molar Mass Polymers by Metal-Catalyzed Living Radical Polymerization of Acrylates, Methacrylates, and Vinyl Chloride Mediated by SET at 25 °C. *J. Am. Chem. Soc.* **2006**, *128*, 14156−14165.
(27) Debuigne, A.; Hurtgen, M.; Detrembleur, C.; Jérôme, C.; Barner-Kowollik, C.; Junkers, T. Interpolymer radical coupling: A toolbox complementary to controlled radical polymerization. *Prog. Polym. Sci.* **2012**, *37*, 1004−1030.
(28) Nakamura, Y.; Ogihara, T.; Yamago, S. Mechanism of Cu(I)/Cu(0)-Mediated Reductive Coupling Reactions of Bromine-Terminated Polyacrylates, Polymethacrylates, and Polystyrene. *ACS Macro Lett.* **2016**, *5*, 248−252.
(29) Matyjaszewski, K.; Woodworth, B. E.; Zhang, X.; Gaynor, S. G.; Metzner, Z. Simple and Efficient Synthesis of Various Alkoxyamines for Stable Free Radical Polymerization. *Macromolecules* **1998**, *31*, 5955−5957.
(30) Yoshikawa, C.; Goto, A.; Fukuda, T. Reactions of polystyrene radicals in a monomer-free atom transfer radical polymerization system. *e-Polym.* **2002**, *2*, 172−183.
(31) Sarbu, T.; Lin, K.-Y.; Ell, J.; Siegwart, D. J.; Spanswick, J.; Matyjaszewski, K. Polystyrene with Designed Molecular Weight Distribution by Atom Transfer Radical Coupling. *Macromolecules* **2004**, *37*, 3120−3127.
(32) Voter, A. F.; Tillman, E. S. An Easy and Efficient Route to Macrocyclic Polymers Via Intramolecular Radical−Radical Coupling of Chain Ends. *Macromolecules* **2010**, *43*, 10304−10310.
(33) Blackburn, S. C.; Myers, K. D.; Tillman, E. S. Macrocyclic poly(methyl acrylate) and macrocyclic poly(methyl acrylate-*block*-styrene) synthesized by radical trap-assisted atom transfer radical coupling. *Polymer* **2015**, *68*, 284−292.
(34) Carnicom, E. M.; Tillman, E. S. Polymerization of styrene and cyclization to macrocyclic polystyrene in a one-pot, two-step sequence. *React. Funct. Polym.* **2014**, *80*, 9−14.
(35) Voter, A. F.; Tillman, E. S.; Findeis, P. M.; Radzinski, S. C. Synthesis of Macrocyclic Polymers Formed via Intramolecular Radical Trap-Assisted Atom Transfer Radical Coupling. *ACS Macro Lett.* **2012**, *1*, 1066−1070.
(36) Harth, E.; Van Horn, B.; Lee, V. Y.; Germack, D. S.; Gonzales, C. P.; Miller, R. D.; Hawker, C. J. A Facile Approach to Architecturally Defined Nanoparticles via Intramolecular Chain Collapse. *J. Am. Chem. Soc.* **2002**, *124*, 8653−8660.
(37) Chiefari, J.; Chong, Y. K.; Ercole, F.; Krstina, J.; Jeffery, J.; Le, T. P. T.; Mayadunne, R. T. A.; Meijs, G. F.; Moad, C. L.; Moad, G.; Rizzardo, E.; Thang, S. H. Living Free-Radical Polymerization by Reversible Addition−Fragmentation Chain Transfer: The RAFT Process. *Macromolecules* **1998**, *31*, 5559−5562.
(38) Li, W.; Chung, H.; Daeffler, C.; Johnson, J. A.; Grubbs, R. H. Application of 1H DOSY for Facile Measurement of Polymer Molecular Weights. *Macromolecules* **2012**, *45*, 9595−9603.
(39) Ormategui, N.; Garcia, I.; Padro, D.; Cabanero, G.; Grande, H. J.; Loinaz, I. Synthesis of single chain thermoresponsive polymer nanoparticles. *Soft Matter* **2012**, *8*, 734−740.
(40) Edward, J. T. Molecular volumes and the Stokes-Einstein equation J. *J. Chem. Educ.* **1970**, *47*, 261−270.
(41) Bernal-García, J. M.; Guzmán-López, A.; Cabrales-Torres, A.; Estrada-Baltazar, A.; Iglesias-Silva, G. A. Densities and Viscosities of (N,N-Dimethylformamide + Water) at Atmospheric Pressure from (283.15 to 353.15) K. *J. Chem. Eng. Data* **2008**, *53*, 1024−1027.

DOI: 10.1021/acs.macromol.7b00497
Macromolecules XXXX, XXX, XXX−XXX